

Mathematical Modeling Using ANN Based on k-fold Cross Validation Approach and MOAHA Multi-Objective Optimization Algorithm During Turning of Polyoxymethylene POM-C

Tallal Hakmi^{1,*}, Amine Hamdi¹, Aissa Laouissi², Hammoudi Abderazek²,
Salim Chihaoui³, Mohamed Athmane Yallese³

¹ Laboratory of Mechanical Engineering, Materials and Structures, Tissemsilt University, 38000, Algeria

² Mechanics Research Centre, P.B. 73B, 25021, Constantine, Algeria

³ Mechanics and Structures Research Laboratory (LMS), May 8th 1945 University, Guelma 24000, Algeria

Received 18 Sep 2023

Accepted 26 Nov 2023

Abstract

The paper has a dual purpose: firstly, to examine the influence of various cutting conditions (cutting speed V_c , feed f , depth of cut ap , tool nose radius r_e , and cutting edge angle X_r) on the quality of machined parts (Ra), tangential force (F_z) and cutting power (P_c) during the turning process of polyoxymethylene POM-C. Two carbide inserts, SPMR 120304 and SPMR 120308, were used for the three-dimensional cutting operations. Secondly, the goal is to identify optimal cutting conditions that maximize material removal rate (MRR) while minimizing three output parameters (Ra , F_z , and P_c). The study employed analysis of variance (ANOVA) to assess the significance of the input parameters on the desired outcomes and utilized an artificial neural network (ANN) to create mathematical models. The K-fold Cross-Validation approach was deemed suitable due to its efficiency in requiring fewer experiments. To optimize the cutting conditions, a new metaheuristic optimization algorithm called Multi-Objective Artificial Hummingbird Algorithm (MOAHA) was selected. ANOVA analysis reveals that factors f and r_e contribute 58.05% and 32.25%, respectively, to the response Ra . Classical parameters (V_c , f , and ap) also impact mechanical cutting actions (F_z and P_c). The MOAHA algorithm, coupled with four ANN models, optimized the five cutting conditions, resulting in optimal values $V_c = 250 \text{ m/min}$, $f = 0.08 \text{ mm/rev}$, $ap = 1.3 \text{ mm}$, $r_e = 0.8 \text{ mm}$, and $X_r = 75^\circ$. Under these conditions, responses are: $Ra = 0.6 \mu\text{m}$, $F_z = 21.51 \text{ N}$, $P_c = 60.24 \text{ W}$, and $MRR = 26.38 \text{ cm}^3/\text{min}$. The ANN-MOAHA coupling provides an excellent, simple, and fast computer tool for multi-objective optimization.

© 2024 Jordan Journal of Mechanical and Industrial Engineering. All rights reserved

Keywords: Polyacetal POM-C, Turning, ANN, K-Fold Cross-Validation, MOAHA.

Abbreviations

ANN: Artificial neural network
MOAHA: Multi-Objective Artificial Hummingbird Algorithm
POM-C: Polyoxymethylene (polyacetal)
ANOVA: Analysis of variance
 MRR : Material removal rate
IHSA : Improved harmony search algorithm
RSM: Response surface methodology
DF: Desirability function
 Ra : Arithmetic mean roughness
 R_t : Maximum peak to valley height
 R_z : Mean roughness depth
 F_z : Cutting force
 P_c : Cutting power

1. Introduction

Polymeric materials are increasingly prevalent in mechanical engineering applications like automotive,

aerospace, optics, robotics, and machinery [1, 2]. In the automotive sector, these materials are utilized for creating intricate components such as gears, racks, wheels, bearings, transmission pinions, valve seats, and more [3]. They offer several advantages in these applications, including excellent formability, moldability, good mechanical properties, affordability, lightweight, high resistance to corrosion and wear, durability in aggressive environments, noiseless operation without the need for lubrication, dimensional stability, and rigidity [3–5]. Consequently, they provide a compelling alternative to traditional metals, reducing production costs in various applications. In plastics processing, extrusion is a commonly employed method for both thermoplastics and thermosets. Mass production typically involves molding techniques for engineering plastics. However, components produced via shaping processes (like molding and forming) often necessitate additional machining to meet

* Corresponding author e-mail: talal.hakmi@univ-tissemsilt.dz.

industry requirements for dimensional accuracy and surface quality [1,3, 6, 7].

Several studies have delved into the machining of various engineering plastics [8–10]. Jasper et al. [8] examined the turning of glass fiber reinforced plastic (GFRP) considering standard cutting parameters (V_c , f , and ap). Their experimental results, obtained through a Taguchi L_9 experimental design, reveal that the feed primarily influences surface roughness. Additionally, cutting speed emerges as the key factor affecting machining time, while depth of cut is the primary control parameter impacting material removal rate (MRR). Madić et al. [11, 12] employed artificial neural networks (ANNs), the simplex method, improved harmony search algorithm (IHSA), and Taguchi L_{27} design to model and optimize the surface roughness (Ra) when turning PA-6 polyamide. The authors suggest that minimal surface roughness is likely achieved when the three classical cutting parameters (V_c , f , and ap) are kept small, and the other tool parameter (r_e) is set to a larger value.

In the literature on machining polymer materials, Chabbi et al. [13, 14] conducted an empirical and statistical investigation to assess the impact of cutting parameters (V_c , f , and ap) when turning POM-C. They used a comprehensive factorial design (L_{27}) and the carbide cutting tool SCMN 120408 (K10) for their experiments. The parameters under scrutiny were Ra , F_i , P_c , and MRR , with statistical analysis relying on RSM, ANN, and DF techniques. In summary, the results revealed that surface roughness is predominantly affected by the feed, contributing 66.41%, followed by ap at 19.70%, with V_c having a lesser impact. In contrast, tangential cutting force (F_z) is influenced by both ap and f , contributing 45.41% and 31.09%, respectively. The third response, P_c , is determined by three factors: ap , f , and V_c , contributing 47.81%, 30.50%, and 12.63%, respectively. In a recent study, Bertolini et al. [7] examined the surface quality of biomedical-grade polyetheretherketone (PEEK) using dry and cryogenic turning processes. The study demonstrated that cryogenic turning consistently results in superior surface quality compared to the dry state. To understand the impact of two factors, V_c and f , on Ra and Rt during the turning of glass fiber reinforced plastic (GFRP) and polyetherketone reinforced with 30% glass fiber (PEEK GF 30), Paulo Davim et al. [15, 16] conducted statistical analyses (ANOVA). All experimental tests and survey results highlighted that the feed is the primary factor influencing the arithmetic mean roughness Ra , contributing 65.9% and 99.1%, respectively.

In the literature, several studies [17–21] have explored the impact of machining conditions on engineering plastics, focusing on output parameters like surface texture, cutting temperature, material removal rate, viscous deformation, crystallinity rate, cutting forces, and cutting power. A recent study by Azzi et al. [17] determined that the optimal parameters for minimizing Ra and maximizing MRR during the turning of polytetrafluoroethylene polymer (PTFE) are $ap = 2 \text{ mm}$, $f = 0.126 \text{ mm/rev}$, and $V_c = 270 \text{ m/min}$. They found that the key influencer for the quantities of interest (Ra , Rz , and MRR) is the feed, with contributions of 90.02%, 91.81%, and 49.22%, respectively. Furthermore, Lazarević et al. [22] employed analysis of variance (ANOVA) and the Taguchi L_{27}

method to optimize cutting parameters (V_c , f , ap , and r_e) when turning PA-6 polyamide. The primary objective was to minimize arithmetic roughness Ra , with the factors ranked in terms of significance as f , r_e , and ap . The impact of interactions and cutting speed V_c was found to be negligible. Jagtap et al. [23] delved into the effect of turning parameters on the surface flatness of both nylon and polypropylene. Their findings highlighted that the feed is the most influential factor for flatness in both polymers. Despite this, the minimum flatness value for polypropylene ($10.7 \mu\text{m}$) remains lower than that of nylon ($16.65 \mu\text{m}$). Similarly, Keddeche et al. [24] presented a statistical analysis of three output parameters: surface roughness, cutting forces, and cutting temperature, during dry turning of polyethylene pipes (HDPE-100 and HDPE-80) using GC3015 carbide inserts (K10). They utilized Taguchi L_9 design and ANOVA to ascertain the effect of cutting parameters (V_c , f , and ap) on these responses. Decreasing the feed leads to improvements in all three surface parameters for both types of polyethylene (Ra , Rt , and Rz), while increasing cutting speed results in a decrease in all three cutting force components (F_r , F_a , and F_z). Additionally, the depth of cut was found to significantly influence cutting temperature. In a recent study, Hamdi et al. [25] demonstrated that feed (f) and the use of minimal quantity lubrication (MQL) are two independent factors that influence specific cutting energy (SCE) consumption during CNC turning of unreinforced polypropylene (PP).

Nevertheless, few papers have been made to investigate the effect of cutting conditions, on output parameters during polymer turning. So far, the influence of cutting tool parameters (r_e and X_r) on the turning of polyoxymethylene POM-C have not been studied. Therefore, the main objective of this paper was to study the effect of cutting parameters (V_c , f , ap , r_e , and X_r) on machined part quality (Ra), cutting force (F_z), cutting power (P_c) and productivity (MRR) in POM-C polyacetal turning. The measured values of the responses were used to determine the four mathematical models by the artificial neural network approach (ANN). The latter was coupled with K-fold cross validation to give more reliability to ANN models. In the last part, these models were integrated with the Multi-Objective Artificial Hummingbird Algorithm (MOAHA) to optimize the cutting conditions to maximize productivity (MRR) and minimize other responses (Ra , F_z , and P_c). In the next paragraph, the experimental method will be presented.

2. Experimental procedure

2.1. Workpiece material, cutting insert and tool holder

Turning operations for assessing surface roughness, cutting forces, and cutting power were performed on POM-C polyoxymethylene workpieces sourced from Ensinger. These workpieces had an 80 mm diameter and a 300 mm length. Polyacetal, a semi-crystalline thermoplastic, boasts impressive characteristics, including excellent corrosion resistance, low moisture absorption, high abrasion resistance, and a balanced combination of toughness, wear resistance, and rigidity. POM-C's

qualities, like strong dimensional stability and resistance to stress, make it a versatile material suitable for various applications, including the production of intricate components like gears, contacting rollers, bearings, and wheels. You can find mechanical and thermal properties of this lightweight material in Table 1.

Table 1. Mechanical and thermal properties of POM-C polyacetal

Properties	Values	Standards
Density	1.41 g/cm ³	DIN EN ISO 1183
Tensile modulus of elasticity	2800 MPa	DIN EN ISO 527-2
Flexural modulus of elasticity	2600 MPa	DIN EN ISO 178
Resistance to traction	67 MPa	DIN EN ISO 527-2
Resistance to flexion	91 MPa	DIN EN ISO 178
Brinell hardness	165 MPa	ISO 2039-1
Melting temperature	166 °C	DIN 53765
Operating temperature	100 °C	DIN 53765
Heat conductivity	0.39 W/m*k	ISO 22007-4 :2008

The machine-tool used in the experimental tests was a "TOS TRENCIN" parallel lathe, model SN40C with equal spindle power of 6.6 kW. Furthermore, two carbide inserts SPMR 120304 ($r_e = 0.4 \text{ mm}$) and SPMR 120308 ($r_e = 0.8 \text{ mm}$) from the company Dormer Pramet were used in order to perform the three-dimensional cutting operations. Machining this type of material requires strongly positive cutting angle values. Moreover, two tool holders were employed to mount the inserts, the designation according to ISO is CSDPN 2525M12 ($X_r = 45^\circ$) and CSBPR 2525M12 ($X_r = 75^\circ$).

2.2. Measurement configuration

The arithmetic mean roughness (Ra) is measured by a Mitutoyo SurfTest-201 roughness meter equipped with a stylus diamond tip of radius $5 \mu\text{m}$. Furthermore, evaluation length $L_n = 2,4 \text{ mm}$, Gaussian filter and cut-off $\lambda_c = 0,8 \text{ mm}$ were used. Each test was characterized by three measurements in different locations separated by an angle of 120° and the average value was taken to give more reliability to the results. The tangential cutting force was measured with a Kistler piezoelectric dynamometer (model 9257B), the latter was connected by a multi-channel charge amplifier (type 5011B). Figure 1 summarizes the procedures followed to carry out this paper.

2.3. Design of experiments (DOE)

In the turning process, an important number of independent variables influence one or more responses, i.e., the cutting parameters variables, the cutting tool parameters and those of the machined part. In this paper,

the machining parameters chosen were as follows: cutting speed (V_c), feed (f), depth of cut (ap), tool nose radius (r_e), and cutting edge angle (X_r). The selected factors and their levels are shown in Table 2. The cutting conditions ranges have been selected from the recommendations of cutting tool manufacturer Dormer Pramet and POM-C manufacturer Ensinger. In order to fix and reduce the number of experiments compared to the full factorial design (FFD), the Taguchi multifactorial method ($L_{16} = 4^3 \times 2^2$) was chosen. This technique reduces the time and cost of carrying out experiments.

Table 2. Cutting conditions and their levels

	Level 1	Level 2	Level 3	Level 4
$V_c (m/min)$	240	300	360	420
$f (mm/rev)$	0.08	0.14	0.20	0.24
$ap (mm)$	0.8	1.6	2.4	3.2
$r_e (mm)$	0.4	0.8	–	–
$X_r (^\circ)$	45	75	–	–

3. Results and discussion

The experimental results of $Ra (\mu\text{m})$, $F_z (N)$, P_c , and MRR corresponding to the levels of the selected cutting parameters (V_c , f , ap , r_e , and X_r) following the Taguchi L_{16} design are shown in Table 3. The material removal rate (MRR in cm^3/min) and cutting power (P_c in W) are calculated by equations. 1 and 2.

$$MRR = V_c \times f \times ap \quad (1)$$

$$P_c = \frac{F_z \times V_c}{60} \quad (2)$$

According to Table 3, the minimum and maximum values of the experimental results vary between $0.60 \mu\text{m}$ to $5.05 \mu\text{m}$ for Ra , 13.56 N to 113.04 N for F_z , $15.36 \text{ cm}^3/\text{min}$ to $192.00 \text{ cm}^3/\text{min}$ for MRR , and 54.24 W to 527.80 W for P_c . Experiment number 13 exhibits the most favorable combination of acceptable values for Ra , F_z , P_c , and MRR . These results are employed in sections devoted to analysis of variance (ANOVA), modeling, and optimization. Consequently, a comprehensive discussion and detailed analysis will follow.

3.1. Statistical analysis using ANOVA

ANOVA is a statistical method that follows probability and mathematics rules to provide an analysis and interpretation of experimental data. The main purpose of this mathematical tool is to verify the validity of the models. Moreover, this approach allows to determine the influence of the input parameters on the response variation. ANOVA was performed with a 95% confidence interval (significance level: $\alpha = 0.05 = 5\%$). A model, independent variable or interaction can be significant or not when the probability value p is [26–29]:

- If the value of $p \leq 0.05$, the parameter is significant,
- If the value of $p > 0.05$, the parameter is insignificant.

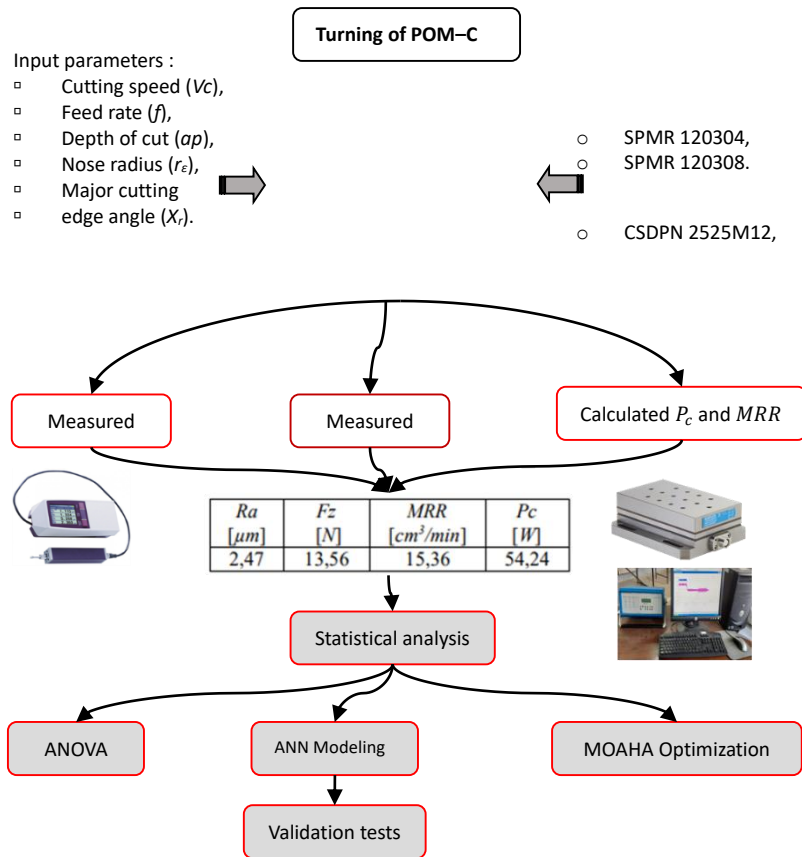


Figure 1. Flowchart of the experimental configuration

Table 3. Experimental results of $Ra(\mu m)$, $F_z (N)$, $MRR (cm^3/min)$, and $P_c(W)$ as a function of cutting conditions

N	Input factors					Output parameters			
	V_c	f	ap	r_ϵ	X_r	Ra	F_z	MRR	P_c
1	240	0.08	0.8	0.4	45	2.47	13.56	15.36	54.24
2	240	0.14	1.6	0.4	45	3.10	45.65	53.76	182.60
3	240	0.20	2.4	0.8	75	2.15	80.71	115.20	322.84
4	240	0.24	3.2	0.8	75	2.92	113.04	184.32	452.16
5	300	0.08	1.6	0.8	75	1.01	24.20	38.40	121.00
6	300	0.14	0.8	0.8	75	1.30	25.30	33.60	126.50
7	300	0.20	3.2	0.4	45	4.00	105.56	192.00	527.80
8	300	0.24	2.4	0.4	45	5.05	88.67	172.80	443.35
9	360	0.08	2.4	0.4	75	1.35	38.22	69.12	229.32
10	360	0.14	3.2	0.4	75	2.35	75.30	161.28	451.80
11	360	0.20	0.8	0.8	45	2.52	24.90	57.60	149.40
12	360	0.24	1.6	0.8	45	2.99	65.30	138.24	391.80
13	420	0.08	3.2	0.8	45	0.60	59.71	107.52	417.97
14	420	0.14	2.4	0.8	45	1.32	60.12	141.12	420.84
15	420	0.20	1.6	0.4	75	3.27	49.14	134.40	343.98
16	420	0.24	0.8	0.4	75	3.98	35.25	80.64	246.75

Tables 4–6 describe the ANOVA of the dependent variables (Ra , F_z , and P_c) in terms of the independent variables (V_c , f , ap , r_ϵ , and X_r).

3.1.1. Surface roughness (Ra)

The quality of precision mechanical parts relies heavily on the surface finish achieved through various machining processes. In this context, the key parameter for evaluating the quality of parts produced through well-defined edge processes, like turning, is the arithmetic mean roughness Ra . Analyzing the ANOVA results for Ra in Table 4 reveals that the most influential factor impacting surface roughness is the feed, contributing over 50%. The nose radius r_ϵ is the second most significant factor, with a

32.25% contribution. As for the other parameters, cutting speed V_c and cutting edge angle X_r are statistically significant but have relatively modest effects, contributing 2.40% and 3.86%, respectively. Interestingly, ap does not significantly affect Ra . These findings align with those reported by Chabbi et al. [13, 14] during their study on POM-C turning. Furthermore, Pradeep Allu et al. [30] observed similar results when turning AISI 52100 hard steel.

3.1.2. Tangential force (F_z)

In this paper, the study and evaluation of the cutting mechanical actions during the turning of polyacetal POM-C is represented by the tangential cutting force (F_z) and the cutting power (P_c). The results of the ANOVA for F_z are presented in Table 5. This table shows that the depth of cut is the first factor influencing F_z by a percentage of 66.48%, followed by the feed with a contribution of 28.69%, while the cutting speed is the last significant parameter with a low percentage of 3.21%. The other two input parameters are not significant because these probability values are greater than 0.05. According to Laouissi et al. [31], these results are in agreement with the theory that correlates the cutting force F_z with the two factors ap and f respectively. In this regard, similar results were found by Nouioua et al. [32] when turning X210CR12 steel with minimum quantity lubrication (MQL). Along these lines, Laouissi et al. [33] reported that the cutting force is largely influenced by the three factors ap , f , V_c , and the interaction ($ap \times f$) when turning EN-GJL-250 gray iron with coated and uncoated silicon nitride ceramics (Si_3N_4).

3.1.3. Cutting power (P_c)

The analysis of variance of the cutting power P_c is given in Table 6. Through this table, the contribution of the depth of cut is the highest (67.81%), which shows that it is the factor that most influences the P_c response. The next factor influencing the cutting power is the feed f , followed by the cutting speed V_c , with contributions of 20.57% and 6.09%, respectively. Regarding the cutting

tool parameters, it can be seen that both factors (r_e and X_r) have a non-significant effect, i.e., a sum of contribution less than 2%. Comparison of the ANOVA results for F_z and P_c clearly shows that these two responses are affected by the same input parameters (ap , f , and V_c). The same conclusion was found by Chabbi et al. [13, 14] and Laouissi et al. [34].

3.2. ANN-based modeling

A neural network is an adaptable system that can learn relationships through repeated exposure to data and is capable of generalizing to new, previously unseen data [35]. The idea behind ANNs is to emulate the brain's functioning to solve technical problems that may not be solvable using other methods, as noted by Svorcan et al. [36]. Thus, ANN serves as a decision support tool [37]. The use of ANNs has reduced the development time and enhanced the flexibility of the studied system [38]. In the realm of mechanical material removal processes, the ANN algorithm is the most commonly used artificial intelligence approach, according to Panadiyan et al. [39]. It is a sophisticated mathematical and computer science method that establishes a mathematical relationship between a response variable (Y) and one or more independent variables (X_i , where i can be 1, 2, ..., n). In recent years, researchers in various fields, such as prediction of friction stir welding [40], hard turning [41], turning process [42], machine condition monitoring [43], drilling process [44], electrical discharge machining process [45], extensively use ANN modeling, which underlines the importance of this mathematical technique in material removal machining.

Table 4. ANOVA for Ra

Source	DF	SC	MC	F	Prob.	Cont.%	Remarks
V_c	1	0.5379	0.5379	7.31	0.022	2.40	Significant
f	1	13.0238	13.0238	177.02	<0.0001	58.05	Significant
ap	1	0.0361	0.0361	0.49	0.499	0.16	Insignificant
r_e	1	7.2361	7.2361	98.35	<0.0001	32.25	Significant
X_r	1	0.8649	0.8649	11.76	0.006	3.86	Significant
Residual	10	0.7357	0.0736				
Cor total	15	22.4346					

Table 5. ANOVA for F_z

Source	DF	SC	MC	F	Prob.	Cont.%	Remarks
V_c	1	433.5	433.52	23.17	0.001	3.21	Significant
f	1	3871.3	3871.28	206.94	<0.0001	28.69	Significant
ap	1	8972.5	8972.48	479.62	<0.0001	66.48	Significant
r_e	1	0.2	0.23	0.01	0.913	0.00	Insignificant
X_r	1	31.1	31.11	1.66	0.226	0.23	Insignificant
Residual	10	187.1	18.71				
Cor total	15	13495.7					

Table 6. ANOVA for P_c

Source	DF	SC	MC	F	Prob.	Cont.%	Remarks
V_c	1	19743	19743	16.19	0.002	6.09	Significant
f	1	66724	66724	54.71	<0.0001	20.57	Significant
ap	1	220027	220027	180.42	<0.0001	67.81	Significant
r_e	1	374	374	0.31	0.592	0.12	Insignificant
X_r	1	5389	5389	4.42	0.062	1.66	Insignificant
Residual	10	12195	1220				
Cor total	15	324452					

ANNs consist of three interconnected layers: the input layer, the hidden layer, and the output layer (see figure2)[46]. The input layer is where the factor values are introduced. The hidden layer processes the relationships between the independent variables from the previous layer. The output layer presents the results of the intermediate layer as mathematical equations. The back propagation algorithm (BPA) based on gradient descent is used during the network learning stage. The hyperbolic tangent function (f) is the activation function employed in this study. The ideal neural architecture for the three responses is 5-3-1, meaning it has an input layer with 5 nodes, a single hidden layer with 3 nodes, and an output layer with 1 node. This configuration helps the model effectively capture essential features, process them, and provide accurate responses. The balanced architecture ensures optimal performance for the specific problem being addressed. The activation function is crucial for ANN, as it determines their ability to model a system.

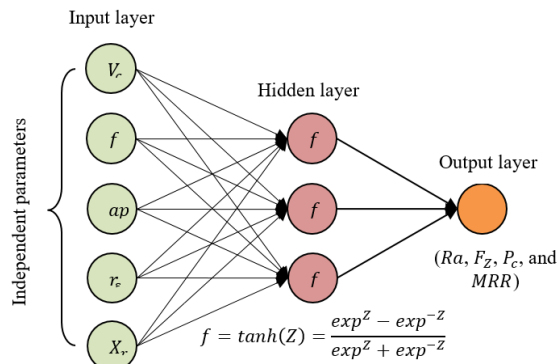


Figure 2. Artificial neural network architecture.

3.2.1. ANN with K-fold cross validation

After training an ANN model on labeled data, it is assumed to work on new data. However, it is important to ensure the accuracy of the model predictions in production. To do this, it is necessary to validate the model. The validation process involves deciding whether the numerical results quantifying the hypothesized relationships between the variables are acceptable as descriptions of the data.

One of the techniques used to test the effectiveness, performance and quality of an ANN model is K-fold cross validation. Furthermore, this method is a re-sampling procedure to evaluate a model even with limited data [47]. The K-Fold technique is simple to understand, and particularly popular. Compared to other Cross-Validation approaches, it generally results in a less biased model. This is because this method ensures that all observations in the original data set have a chance to appear in both the training and test sets. Therefore, in case of limited input data, it constitutes one of the best approaches. According to Ming et al. [48], the ANN model with K-fold cross-validation gives a better prediction result compared to the stand-alone ANN model.

The first step of this technique is to separate the data set randomly into K-fold. Thus, the procedure has a single parameter called K referring to the number of groups into

which the sample will be divided. In this perspective, the choice of the value of K is determined according to the length of the dataset (neither too low nor too high) [49]. In our case, $K = 4$, i.e., the dataset of our study will be divided into 4 sections (see figure3). Then, in turn, we learn on a fold and test on the others. The process is repeated until each K-fold serves within the training set. The average of the recorded scores is the performance metric of the model.

	Fold 1	Fold 2	Fold 3	Fold 4
ANN 1	Testing	Training	Training	Training
ANN 2	Training	Testing	Training	Training
ANN 3	Training	Training	Testing	Training
ANN 3	Training	Training	Training	Testing

Data set languor

Figure 3. Choice of the K value according to the length of the dataset.

The obtained mathematical models of Ra , F_z , P_c , and MRR as a function of the input parameters (V_c , f , ap , r_c , and X_r) using the ANN technique with K-fold cross validation and their coefficients of determination (R^2) are presented by equations 3–6. The R^2 values are very close to unity ($R^2 = 0.99$ for all four models). This means that the models developed by the ANN technique with K-fold cross validation are statistically significant, which demonstrates a strong correlation between the experimental data and the prediction results.

3.2.2. Comparison between experimental and ANN predicted values

Figure 4 shows the comparison between the experimental values of the responses (Ra , F_z , and P_c) and the results predicted by the ANN mathematical models. This comparison confirms the strong correlation between the experimental data and the predicted values as all points are very close. The mean absolute percentage error (MAPE) values of the dependent variables (Ra , F_z , and P_c) are 3.82%, 6.49% and 5.96% respectively. Thus, these ANN models can be used to predict the values of the previous four responses within the range of the turning parameters selected in Table 2.

3.2.3. Validation tests

In general, the experimental values used to build the model have errors. These are passed on to the model coefficients and then to the values calculated by the model. To this end, four additional experimental validation tests were performed to verify the quality and performance of the models developed by ANN. The cutting conditions are selected within their range in Table 2. From the results shown in Table 7, the values of the absolute prediction error (APE) are in the ranges 2.61%-17.51% for the surface roughness Ra , 4.19%-8.01% for the cutting force F_z , 0.24%-8.16% for the cutting power P_c and 0.44%-19.26% for the material removal rate MRR . These results confirm the performance and reliability of the four models to predict new results within the range of cutting conditions when turning POM-C, as shown in Table 2.

$$Ra = 0.80328H_1 - 0.86417H_2 + 3.42147H_3 + 3.35752 \tag{3}$$

$$R_{Ra}^2 = 0.99986$$

Where:

$$\begin{cases} H_1 = \tanh(0.5(-0.00768V_c + 3.7979f - 0.651ap - 1.3423r_\epsilon + 0.03102X_r + 2.6805)) \\ H_2 = \tanh(0.5(0.0072V_c + 1.16324f - 0.3428ap - 1.3113r_\epsilon + 0.0654X_r - 5.84277)) \\ H_3 = \tanh(0.5(0.00154V_c + 10.791f + 0.04807ap - 2.5646r_\epsilon - 0.0034X_r - 1.58929)) \end{cases}$$

$$F_Z = 53.45295H_1 - 16.55734H_2 - 66.0027H_3 + 78.24948 \tag{4}$$

$$R_{F_Z}^2 = 0.99871$$

Where:

$$\begin{cases} H_1 = \tanh(0.5(0.00766V_c + 7.47738f + 0.72136ap + 0.22988r_\epsilon - 0.01906X_r - 4.79437)) \\ H_2 = \tanh(0.5(-0.01345V_c - 2.21095f - 0.03403ap + 0.42603r_\epsilon - 0.01573X_r + 5.95418)) \\ H_3 = \tanh(0.5(0.01129V_c - 3.48000f - 0.383260ap - 0.09641r_\epsilon - 0.01290X_r - 1.338630)) \end{cases}$$

$$P_c = 91.08569H_1 + 24.8929H_2 - 202.17399H_3 + 256.54684 \tag{5}$$

$$R_{P_c}^2 = 0.99823$$

Where:

$$\begin{cases} H_1 = \tanh(0.5(-0.01964V_c + 17.37462f + 0.86084ap + 3.61084r_\epsilon - 0.00163X_r + 0.71254)) \\ H_2 = \tanh(0.5(0.0031V_c - 42.05361f + 0.40851ap - 4.0589r_\epsilon - 0.01432X_r + 9.31397)) \\ H_3 = \tanh(0.5(-0.01548V_c - 15.48985f - 1.83108ap + 0.37149r_\epsilon - 0.00058X_r + 11.01791)) \end{cases}$$

$$MRR = 49.84269H_1 - 26.60189H_2 + 52.33127H_3 + 116.69902 \tag{6}$$

$$R_{MRR}^2 = 0.99967$$

Where:

$$\begin{cases} H_1 = \tanh(0.5(-0.00416V_c + 26.89733f + 2.059770ap - 5.12039r_\epsilon - 0.03902X_r - 2.9736)) \\ H_2 = \tanh(0.5(-0.01778V_c - 36.76325f + 2.16955ap + 1.52437r_\epsilon + 0.07314X_r + 1.67983)) \\ H_3 = \tanh(0.5(0.01638V_c + 6.105990f + 2.50916ap + 5.19089r_\epsilon + 0.04886X_r - 17.37715)) \end{cases}$$

Table 7. Results of confirmatory tests

N°	V_c	f	ap	r_ϵ	X_r	Experi results	Predic results	APE (%)
Surface roughness Ra (μm)								
1	320	0.16	1	0.4	75	2.59	2.6767	3.23
2	380	0.18	2	0.8	75	1.73	1.4721	17.51
3	280	0.18	1.2	0.4	45	3.72	3.8198	2.61
4	400	0.22	0.8	0.8	45	2.2	2.6347	16.49
Cutting force F_Z (N)								
1	320	0.16	1	0.4	75	30.55	32.1737	5.04
2	380	0.18	2	0.8	75	63.65	58.9278	8.01
3	280	0.18	1.2	0.4	45	33.88	35.4849	4.52
4	400	0.22	0.8	0.8	45	36.59	35.1175	4.19
Cutting power P_c (W)								
1	320	0.16	1	0.4	75	162.93	177.4177	8.16
2	380	0.18	2	0.8	75	403.11	384.8545	4.74
3	280	0.18	1.2	0.4	45	158.1	158.4932	0.24
4	400	0.22	0.8	0.8	45	243.93	229.1617	6.44
Material removal rate MRR (cm^3/min)								
1	320	0.16	1	0.4	75	51.2	42.9287	19.26
2	380	0.18	2	0.8	75	136.8	136.1979	0.44
3	280	0.18	1.2	0.4	45	60.48	66.5560	9.12
4	400	0.22	0.8	0.8	45	70.4	71.8761	2.05

3.3. Cutting parameters optimization by MOAHA

This section deals with the multi-objective optimization of cutting conditions in POM-C polyacetal turning that lead to near optimal values of two or more responses. The empirical ANN models presented in the previous section were used as objective functions. First, constraints on the cutting conditions (V_c , f , ap , r_e , and X_r) were added to the models to confirm that the results are physically significant. In this way, a new metaheuristic optimization algorithm called Multi-Objective Artificial Hummingbird Algorithm (MOAHA) was used. Therefore, the ANN models developed for Ra , F_z , P_c , and MRR were incorporated into the MOAHA algorithm to optimize the cutting conditions.

The artificial hummingbird algorithm (AHA) has been inspired by the foraging behaviors of hummingbirds in nature [50]. It should be noted that this algorithm has been extended to deal with multi-criteria problems by Zhao et al. [51]. Where the authors include three components (an external archive, a dynamic elimination-based crowding distance, and a solution update mechanism) for this purpose. The original version of AHA is based on three main procedures: guided foraging, territorial foraging and migration foraging. In this paper, a multi-objective AHA (MOAHA) is introduced for optimizing the multi-objective machining process during the turning operation. The steps of the MOAHA for this purpose are provided in figure 5.

The MOAHA presents several advantages compared to other algorithms applied in multi-objective optimization. Some of these advantages include solution diversity, adaptability, fast convergence, efficient resource utilization, robustness, and ease of implementation. It is important to note that the benefits of an algorithm often depend on the specific context of the application. However, MOAHA is recognized for its robust performance in various multi-objective optimization problems.

3.3.1. Ra and MRR optimization

Figure 6 shows the values of cutting conditions that minimize surface roughness (Ra) and maximize productivity (MRR). The optimal cutting conditions removed according to this table and figure are $V_c = 359.99 \text{ m/min}$, $f = 0.09 \text{ mm/rev}$, $ap = 2.4 \text{ mm}$, $r_e = 0.8 \text{ mm}$, and $X_r = 75^\circ$. In this sense, the optimal values of these two objective functions are $0.62 \mu\text{m}$ and $67.09 \text{ cm}^3/\text{min}$ respectively. Moreover, this figure clearly shows a proportional relationship between the two responses (Ra and MRR).

3.3.2. F_z and MRR optimization

The couple optimization of MRR and F_z responses are presented by figure 7. The cutting conditions to maximize the objective function MRR and minimize the other function are $V_c = 360 \text{ m/min}$, $f = 0.19 \text{ mm/rev}$, $ap = 1.35 \text{ mm}$, $r_e = 0.4 \text{ mm}$, and $X_r = 75^\circ$. Therefore, the optimal values of these two objective functions are 14.29 N and $113.54 \text{ cm}^3/\text{min}$ respectively. Also, this figure shows the same previous relationship between the two responses (MRR and Ra), which is due to the same

objective considered by the two functions Ra and F_z (minimization).

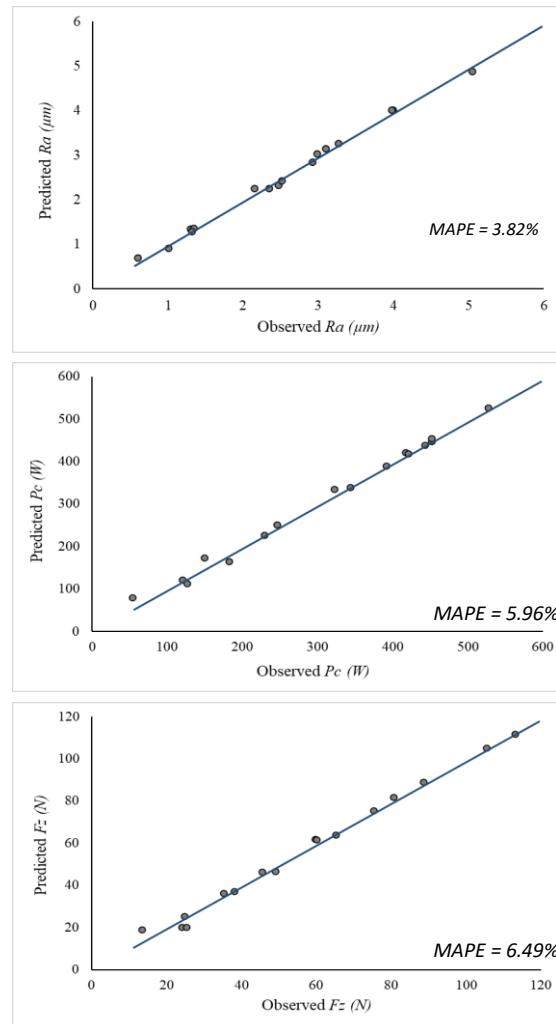


Figure 4. Comparison between the experimental values of the responses (Ra , F_z , and P_c) and the results predicted by the ANN models.

The couple optimization of the Ra and P_c responses are presented by figure 8. The cutting conditions to minimize the two objective functions are as follows: $V_c = 360 \text{ m/min}$, $f = 0.08 \text{ mm/rev}$, $ap = 2.13 \text{ mm}$, $r_e = 0.8 \text{ mm}$, and $X_r = 75^\circ$. Thus, the optimal values of Ra and P_c are $0.6 \mu\text{m}$ and 152.46 W respectively. However, this figure clearly shows an inversely proportional relationship between these two criteria variables, which is due to the opposition of these two endogenous variables.

3.3.3. Combinatorial optimization of the 4 objectives

The optimization of cutting conditions has become a crucial topic in most material removal machining processes. Indeed, the complexity of this part lies in the important number of piloting parameters. Therefore, the goal of this part is to integrate the objectives of the four machining indicators (Ra , F_z , P_c , and MRR) at the same time to determine the optimal cutting parameters. The MOAHA algorithm will be the effective tool of intelligent computing to search for a compromise between several quantities of interest during POM-C turning.

The results of the MOAHA optimization are shown in Table 8. Examination of this table gives the following optimal cutting conditions: cutting speed $V_c = 250.58 \text{ m/min}$, feed $f = 0.08 \text{ mm/rev}$, depth of cut $ap = 1.31 \text{ mm}$, nose radius $r_e = 0.8 \text{ mm}$ and cutting edge angle $X_r = 75^\circ$. In this case, the response values are

$Ra = 0.6 \mu\text{m}$, $F_z = 21.51 \text{ N}$, $P_c = 60.24 \text{ W}$ and $MRR = 26.38 \text{ cm}^3/\text{min}$. In this way, the approach developed by ANN-K-Fold-MOAHA is very effective to optimize the cutting conditions of POM-C turning and to predict the dependent variables (Ra , F_z , MRR , etc).

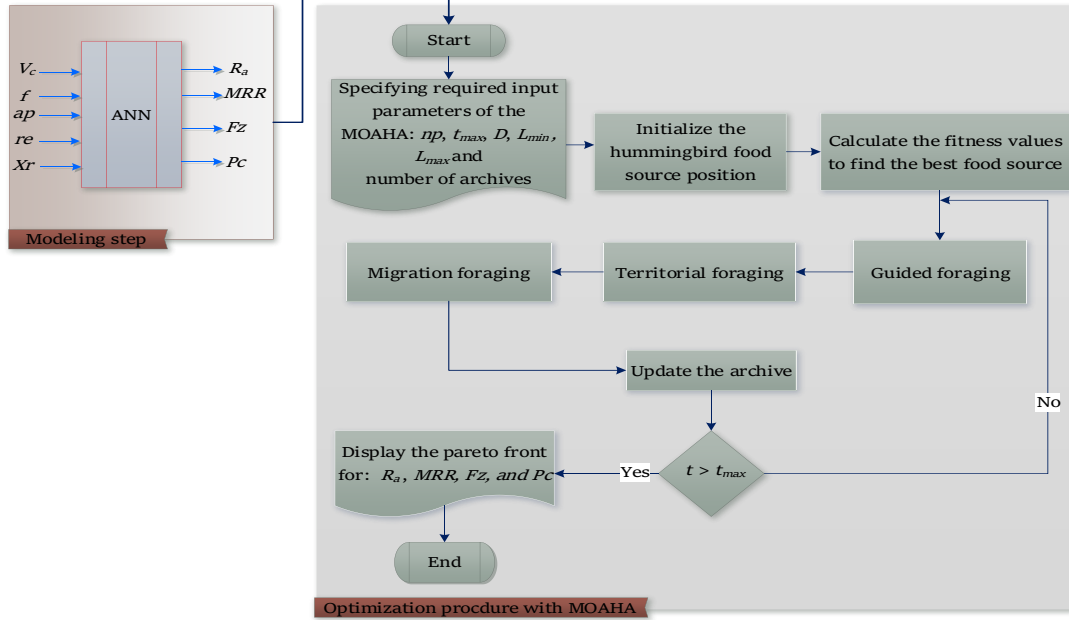


Figure 5. MOAHA for optimization of machining parameters.

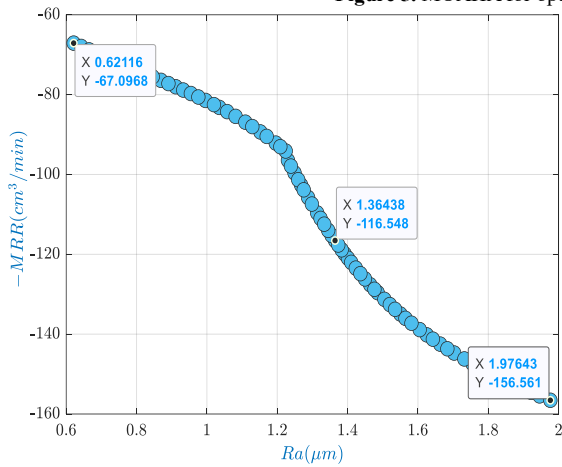


Figure 6. Ra and MRR couple optimization by the MOAHA algorithm.

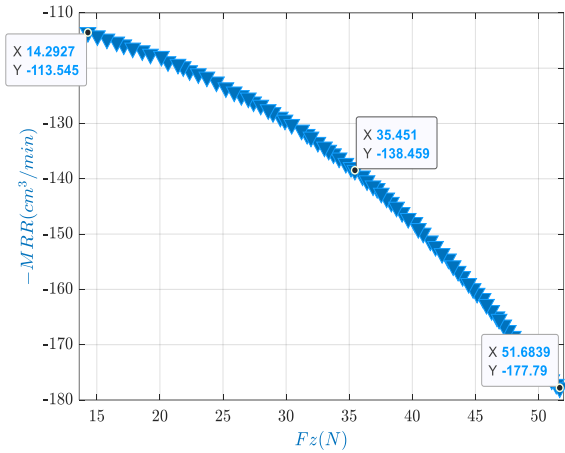


Figure 7. F_z and MRR couple optimization by the MOAHA

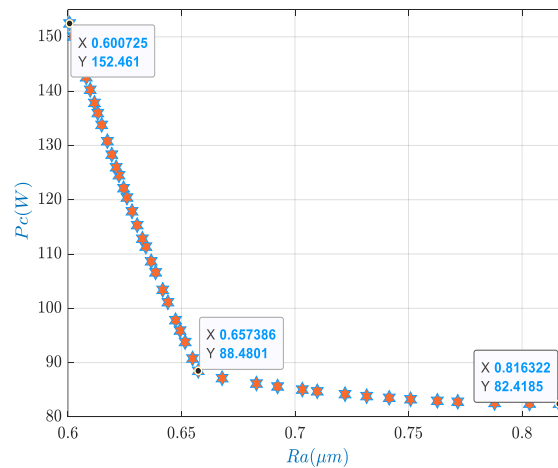


Figure 8. Ra and P_c couple optimization by the MOAHA algorithm.

Table 8. MOAHA optimization results

N°	V_c	f	ap	r_ϵ	X_r	Ra	F_z	MRR	P_c
1	250.58	0.08	1.31	0.8	75	0.60	21.51	26.38	60.24
2	270.86	0.08	1.63	0.8	75	0.61	29.66	37.76	117.89
3	270.91	0.08	1.63	0.8	75	0.62	29.73	37.88	118.21
4	345.84	0.10	1.99	0.8	75	0.63	37.75	70.28	222.73
5	324.30	0.10	1.77	0.8	75	0.74	34.23	60.19	185.10
6	359.99	0.11	1.69	0.8	75	0.8	31.99	69.98	204.40
7	360	0.13	1.69	0.8	75	1.08	36.90	81.72	224.75

4. Conclusions

The objective of this study is to evaluate the influence of cutting conditions (V_c , f , ap , r_ϵ , and X_r) on four quantities of interest (Ra , F_z , P_c , and MRR) when turning POM-C polyacetal. Statistical analysis (ANOVA) and artificial neural network (ANN) with K-fold cross validation approach were used. Thus, the objective is to optimize the cutting conditions in an intelligent way by using a new multi-objective optimization algorithm (MOAHA). The conclusions obtained in this investigation are shown below:

- The analysis of variance (ANOVA) of the quantity of interest Ra indicates that the feed f is the first factor determining this roughness parameter with a contribution greater than 50%, followed by r_ϵ , X_r , and V_c . Their contributions are 32.25%, 3.86% and 2.40%, respectively. Moreover, the use of cutting inserts of large nose radius r_ϵ and a large main direction angle X_r of tool holder improves the surface roughness.
- The mechanical actions of the cut (F_z and P_c) are only influenced by the classical input parameters (V_c , f , and ap). Therefore, the cutting tool parameters (X_r and r_ϵ) are not significant on the cutting force F_z and cutting power P_c . The first factor affecting the two previous responses is the depth of cut (ap) with a contribution of 66.48% and 67.81% respectively, followed by the two factors f and V_c .
- The K-fold cross validation technique is one of the best approaches used to test the efficiency, performance and quality of an ANN mathematical model even with limited data. Indeed, the ANN model with this method gives a better prediction result compared to the standalone ANN model.
- The roughness (Ra), cutting force (F_z), cutting power (P_c) and material removal rate (MRR) models were established by the ANN method with K-fold cross validation. All four models are reliable and in good agreement with the experimental results to estimate the new results in the range of cutting conditions variation.
- The four ANN models were integrated with the MOAHA algorithm to optimize the five cutting conditions. The results found are as follows: $V_c = 250.58 \text{ m/min}$, $f = 0.08 \text{ mm/rev}$, $ap = 1.31 \text{ mm}$, $r_\epsilon = 0.8 \text{ mm}$, and $X_r = 75^\circ$. In this case, the response values are $Ra = 0.6 \mu\text{m}$, $F_z = 21.51 \text{ N}$, $P_c = 60.24 \text{ W}$, and $MRR = 26.38 \text{ cm}^3/\text{min}$.
- The ANN-MOAHA coupling is an effective artificial intelligence tool for finding a good choice of cutting conditions between several quantities of interest from a minimum of experiments. This approach is recommended in the use of industrial mechanics applications in order to estimate the quality of the

machined parts and to optimize the parameters of the machining processes by chip removal.

- Future directions involve implementing the Minimum Quantity Lubrication (MQL) technique for machining POM-C. Additionally, the aim is to assess their sustainability by determining other dependent parameters such as carbon emissions (CO_2), total turning cost (C_{total}), total cutting energy (E_{total}),...etc.

Funding

The present research was received funding from the General Directorate of Scientific Research and Technological Development (DGRSDT), Algerian Ministry of Higher education and Scientific Research (MESRS) under the PRFU research project A11N01UN380120220002.

Conflicts of interest

The authors declare that they have no conflict of interest.

References

- [1] J. Paulo Davim, L.R. Silva, A. Festa and A.M. Abrão, "Machinability study on precision turning of PA66 polyamide with and without glass fiber reinforcing," *Materials and Design*, Vol. 30, 2009, pp.228–234. <https://doi.org/10.1016/j.matdes.2008.05.003>
- [2] J. Paulo Davim and F.A. Mata, "Comparative evaluation of the turning of reinforced and unreinforced polyamide," *Int J Adv Manuf Technol*, Vol. 33, 2007, pp.911–914. <https://doi.org/10.1007/s00170-006-0520-8>
- [3] T.U. Jagtap and H.A. Mandave, "Machining of Plastics A Review," *Int J Eng Res Gen Sci*, Vol.3(2), 2015, pp.577–581.
- [4] F. Mata, P. Reis, J. Paulo Davim, "Physical cutting model of polyamide composites (PA66 GF30)," *Materials Science Forum*, Vols. 514-516, 2006, pp.643–647. <https://doi.org/10.4028/www.scientific.net/MSF.514-516.643>
- [5] J. Paulo Davim, P. Reis, V. Lapa and C. Conceição António, "Machinability study on polyetheretherketone (PEEK) unreinforced and reinforced (GF30) for applications in structural components," *Composite Structures*, Vol. 62, 2003, pp.67–73. [https://doi.org/10.1016/S0263-8223\(03\)00085-0](https://doi.org/10.1016/S0263-8223(03)00085-0)
- [6] R. Keresztes, G. Kalácska, L. Zsidai and Z. Dobrocsi, "Machinability of engineering polymers," *Sustainable Construction and Design*, Vol.2, No.1, 2011, pp.106–114. <https://doi.org/10.21825/scad.v2i1.20467>
- [7] R. Bertolinia, S. Bruschi and A. Ghiotti, "Enhanced surface integrity of a biomedical grade polyetheretherketone through cryogenic machining," *Procedia CIRP*, Vol.102, 2021, pp.488–493. <https://doi.org/10.1016/j.procir.2021.09.083>

- [8] S. Jasper, B. Stalin and M. Ravichandran, "Experimental investigation and Taguchi optimization of turning process parameters for glass fiber reinforced plastics (GFRP)," *International Journal of Advanced Technology and Engineering Exploration*, Vol.5, No.47, 2018, pp.394–399. <http://dx.doi.org/10.19101/IJATEE.2018.547001>
- [9] I. Shyha, D. Huo, P. Hesamikoji, H. Eldessouky and M.A. El-Sayed, "Performance of a new hybrid cutting-abrasive tool for the machining of fibre reinforced polymer composites," *Int J Adv Manuf Technol*, Vol.112, 2021, pp.1101–1113. <https://doi.org/10.1007/s00170-020-06464-7>
- [10] M.S. Kaiser, F. Fazlullah and S.R. Ahmed, "Comparative study of characterization of machined surfaces of some commercial polymeric materials under varying machining parameters," *Journal of mechanical engineering, automation and control systems*, Vol.1, No.2, 2020, pp.75–88. <https://doi.org/10.21595/jmeacs.2020.21643>
- [11] M. Madić, D. Marković and M. Radovanović, "Mathematical modeling and optimization of surface roughness in turning of polyamide based on artificial neural network," *MECHANIKA*, Vol.18, No.5, 2012a, pp.574–581. <https://doi.org/10.5755/j01.mech.18.5.2701>
- [12] M. Madić, D. Marković and M. Radovanović, "Optimization of surface roughness when turning polyamide using ANN-IHSA approach," *International Journal of Engineering and Technology*, Vol.1, No.4, 2012b, pp.432–443. <https://doi.org/10.14419/ijet.v1i4.378>
- [13] A. Chabbi, M.A. Yallese, M. Nouioua, I. Meddour, T. Mabrouki and F. Girardin, "Modeling and optimization of turning process parameters during the cutting of polymer (POM C) based on RSM, ANN, and DF methods," *Int J Adv Manuf Technol*, Vol.91, 2017a, pp.2267–2290. <https://doi.org/10.1007/s00170-016-9858-8>
- [14] A. Chabbi, M.A. Yallese, M. Nouioua, I. Meddour, T. Mabrouki and F. Girardin, "Predictive modeling and multi-response optimization of technological parameters in turning of Polyoxymethylene polymer (POM C) using RSM and desirability function," *Measurement*, Vol.95, 2017b, pp.99–115. <http://dx.doi.org/10.1016/j.measurement.2016.09.043>
- [15] J. Paulo Davim and P. Reis, "Machinability study on composite polyether ether ketone reinforced with 30% glass fibre-PEEK GF 30) using polycrystalline diamond (PCD) and cemented carbide (K20) tools," *Int J Adv Manuf Technol*, Vol.23, 2004a, pp.412–418. <https://doi.org/10.1007/s00170-003-1779-7>
- [16] J. Paulo Davim and F. Mata, "Influence of cutting parameters on surface roughness in turning glass-fibre-reinforced plastics using statistical analysis," *Industrial Lubrication and Tribology*, Vol.56, No.5, 2004b, pp.270–274. <http://dx.doi.org/10.1108/00368790410550679>
- [17] A. Azzi, L. Boulanouar, A. Laouisi, A. Mebrek and M.A. Yallese, "Modeling and optimization of machining parameters to minimize surface roughness and maximize productivity when turning polytetrafluoroethylene (PTFE)," *Int J Adv Manuf Technol*, Vol.123, 2022, pp.407–430. <https://doi.org/10.1007/s00170-022-10160-z>
- [18] C. Fetecau and F. Stan, "Study of cutting force and surface roughness in the turning of polytetrafluoroethylene composites with a polycrystalline diamond tool," *Measurement*, Vol.45, 2012, pp.1367–1379. <https://doi.org/10.1016/j.measurement.2012.03.030>
- [19] N.A. Fountas, I. Ntziantzas and J. Kechagias, "Prediction of cutting forces during turning PA66 GF-30 glass fiber reinforced polyamide by soft computing techniques," *Materials Science Forum*, Vol.766, 2013, pp.37–58. <https://doi.org/10.4028/www.scientific.net/MSF.766.37>
- [20] K.Q. Xiao and L.C. Zhang, "The role of viscous deformation in the machining of polymers," *International Journal of Mechanical Sciences*, Vol.44, 2002, pp.2317–2336. [https://doi.org/10.1016/S0020-7403\(02\)00178-9](https://doi.org/10.1016/S0020-7403(02)00178-9)
- [21] A.I. Alateyah, Y. El-Taybany, S. El-Sanabary, W.H. El-Garaihy and H. Kouta, "Experimental investigation and optimization of turning polymers using RSM, GA, hybrid FFD-GA, and MOGA methods," *Polymers*, Vol.14, No.17, 2022, pp.3585. <https://doi.org/10.3390/polym14173585>
- [22] D. Lazarević, M. Madić, P. Janković and A. Lazarević, "Surface roughness minimization of polyamide PA-6 turning by taguchi method," *Journal of Production Engineering*, Vol.15, 2012, pp.29–32. 2012. <http://www.jpe.ftn.uns.ac.rs/papers/2012/no1/7-Lazarevic.pdf>
- [23] K.A. Jagtap, R.S. Pawade and R. Balasubramaniam, "Some investigations on surface characteristics in precision turning of nylon and polypropylene," 1st International Conference on Recent Trends in Engineering & Technology (2012). <https://ijecscse.org/papers/specialissue/mech/04.pdf>
- [24] M. Kaddeche, K. Chaoui and M.A. Yallese, "Cutting parameter effects on the machining of two high density polyethylene pipes resins," *Mechanics & Industry*, Vol.13, 2012, pp.307–316. <https://doi.org/10.1051/meca/2012029>
- [25] A. Hamdi, Y.F. Yapan, A. Uysal and H. Abderazek, "Multi-objective analysis and optimization of energy aspects during dry and MQL turning of unreinforced polypropylene (PP): an approach based on ANOVA, ANN, MOWCA, and MOALO," *Int J Adv Manuf Technol*, 128, 2023, pp.4933–4950. <https://doi.org/10.1007/s00170-023-12205-3>
- [26] S.A. Rizvi and S.P. Tewari, "Optimization of welding parameters by using Taguchi method and study of fracture mode characterization of SS304H welded by GMAW," *Jordan Journal of Mechanical and Industrial Engineering*, Vol.12, No.1, 2018, pp.17–22.
- [27] Sivarao, K.R. Milkey, A.R. Samsudina, A.K. Dubey and P. Kidd, "Comparison between Taguchi method and response surface methodology (RSM) in modeling CO₂ laser machining," *Jordan Journal of Mechanical and Industrial Engineering*, Vol.8, No.1, 2014, pp.35–42.
- [28] A. Hamdi, S.M. Merghache and T. Aliouane, "Effect of cutting variables on bearing area curve parameters (BAC-P) during hard turning process," *Arch Mech Eng*, Vol.67, No.1, 2020, pp.73–95. <https://doi.org/10.24425/ame.2020.131684>
- [29] M.T. Hayajneh, M.S. Tahat and J. Bluhm, "A study of the effects of machining parameters on the surface roughness in the end-milling process," *Jordan Journal of Mechanical and Industrial Engineering*, Vol.1, No.1, 2007, pp.1–5.
- [30] V. Pradeep Allu, D. Linga Raju and S. Ramakrishna, "Performance investigation of surface roughness in hard turning of AISI 52100 steel - RSM approach," *Materials Today: Proceeding*, Vol.18, 2019, pp.261–269. <https://doi.org/10.1016/j.matpr.2019.06.299>
- [31] A. Laouissi, M. Nouioua, M.A. Yallese, H. Abderazek, H. Maouche and M.L. Bouhalais, "Machinability study and ANN-MOALO-based multi-response optimization during eco-friendly machining of EN-GJL-250 cast iron," *Int J Adv Manuf Technol*, vol.117, 2021, pp.1179–1192. <https://doi.org/10.1007/s00170-021-07759-z>
- [32] M. Nouioua, A. Laouissi, M.A. Yallese, R. Khettabi and S. Belhadi, "Multi-response optimization using artificial neural network-based GWO algorithm for high machining performance with minimum quantity lubrication," *Int J Adv Manuf Technol*, Vol.116, 2021, pp.3765–3778. <https://doi.org/10.1007/s00170-021-07745-5>
- [33] A. Laouissi, M.A. Yallese, A. Belbah, A. Khellaf and A. Haddad, "Comparative study of the performance of coated and uncoated silicon nitride (Si₃N₄) ceramics when machining EN GJL 250 cast iron using the RSM method and 2D and 3D roughness functional parameters," *J Braz. Soc. Mech. Sci.*

- Eng, Vol.41, 2019, pp.205.<https://doi.org/10.1007/s40430-019-1708-9>
- [34] A. Laouissi, M.A. Yaltese, A. Belbah, S. Belhadi and A. Haddad, "Investigation, modeling, and optimization of cutting parameters in turning of gray cast iron using coated and uncoated silicon nitride ceramic tools. Based on ANN, RSM, and GA optimization," *Int J Adv Manuf Technol*, Vol.101, 2019, pp.523–548.<https://doi.org/10.1007/s00170-018-2931-8>
- [35] I. Jalham, "A two-stage artificial neural network model to predict the shrinkage of a polystyrene matrix reinforced with silica sand cement," *Jordan Journal of Mechanical and Industrial Engineering*, Vol.5, No. 3, 2011, pp.255–259.
- [36] J. Svorcan, O. Peković, A. Simonović, et al, "Design of optimal flow concentrator for vertical-axis wind turbines using computational fluid dynamics, artificial neural networks and genetic algorithm," *Advances in Mechanical Engineering*, Vol. 13, No.3, 2021. <https://doi.org/10.1177/1687814021100900>
- [37] Baig, R.U., Javed, S., Khaisar, M., et al., "Development of an ANN model for prediction of tool wear in turning EN9 and EN24 steel alloy," *Advances in Mechanical Engineering*, Vol.13, No.6, 2021, pp.1–14. <https://doi.org/10.1177/16878140211026720>
- [38] N. Lightowler and H. Nareid, "Artificial neural network based control systems," *SAE Technical Paper*, 2003-01-0359, 2003.<https://doi.org/10.4271/2003-01-0359>
- [39] V. Pandiyan, S. Shevchik, K. Wasmer, et al., "Modelling and monitoring of abrasive finishing processes using artificial intelligence techniques: A review," *Journal of Manufacturing Processes*, Vol.57, 2020, pp.114–135. <https://doi.org/10.1016/j.jmapro.2020.06.013>
- [40] Y.K. Yousif, K.M. Daws, B.I. Kazem, "Prediction of friction stir welding characteristic using neural network," *Jordan Journal of Mechanical and Industrial Engineering*, Vol.1, No.1, 2008, pp.43–55.
- [41] A. Hamdi and S.M. Merghache, "Application of artificial neural networks (ANN) and gray relational analysis (GRA) to modeling and optimization of the material ratio curve parameters when turning hard steel," *Int J Adv Manuf Technol*, Vol.124, 2023, pp.3657–3670. <https://doi.org/10.1007/s00170-023-10833-3>
- [42] B.I. Kazem and N.F.H. Zangana, "A neural network based real time controller for turning process," *Jordan Journal of Mechanical and Industrial Engineering*, Vol.2, No.3, 2007, pp.151–155.
- [43] M. Samhouri, A. Al-Ghandoor, S.A. Ali, I. Hinti and W. Massad, "An intelligent machine condition monitoring system using time-based analysis: neuro-fuzzy versus neural network," *Jordan Journal of Mechanical and Industrial Engineering*, Vol.3, No.4, 2009, pp.294–305.
- [44] R. Vinayagamoorthy, N. Rajeswari and B. Karuppiah, "Optimization studies on thrust force and torque during drilling of natural fiber reinforced sandwich composites," *Jordan Journal of Mechanical and Industrial Engineering*, Vol.8, No.6, 2014, pp.385–392.
- [45] J. Anitha, R. Das and M. Kumar Pradhan, "Multi-objective optimization of electrical discharge machining processes using artificial neural network," *Jordan Journal of Mechanical and Industrial Engineering*, Vol.10, No.1, 2016, pp.11–18.
- [46] S.M. Alhaj Ali, A.A. Abu Hammad, M.S. Samhouria and A. Al-Ghandoor, "Modeling stock market exchange prices using artificial neural network: a study of amman stock exchange," *Jordan Journal of Mechanical and Industrial Engineering*, Vol.5, No.5, 2011, pp.439–446.
- [47] Z. Lyu, Y. Yu, B. Samali, M. Rashidi, M. Mohammadi, T.N. Nguyen and A. Nguyen, "Back-propagation neural network optimized by k-fold cross-validation for prediction of torsional strength of reinforced concrete beam," *Materials*, Vol.15, No.4, 2022, pp.1477. <https://doi.org/10.3390/ma15041477>
- [48] J.L.K. Ming, F.S. Taip, M.S. Anuar, S.B.M. Noor and Z. Abdullah, "Artificial neural network topology optimization using k-fold cross validation for spray drying of coconut milk," *IOP Conf. Ser.: Mater. Sci. Eng.* 778 012094, 2020. <https://doi.org/10.1088/1757-899X/778/1/012094>
- [49] A. Laouissi, M.M. Blaoui, H. Abderazek, M. Nouioua and A. Bouchoucha, "Heat treatment process study and annealing based multi-response optimization of c45 steel mechanical properties," *Met. Mater. Int.* Vol.28, 2022, pp.3087–3105. <https://doi.org/10.1007/s12540-022-01197-6>
- [50] W. Zhao, L. Wang and S. Mirjalili, "Artificial hummingbird algorithm: A new bio-inspired optimizer with its engineering applications," *Computer Methods in Applied Mechanics and Engineering*, Vol.388, 2022a, pp.114–194. <https://doi.org/10.1016/j.cma.2021.114194>
- [51] W. Zhao, L. Wang, S. Mirjalili, L. Wang, N. Khodadadi and S.M. Mirjalili, "An effective multi-objective artificial hummingbird algorithm with dynamic elimination-based crowding distance for solving engineering design problems," *Computer Methods in Applied Mechanics and Engineering*, Vol.398, 2022b, pp.115–223. <https://doi.org/10.1016/j.cma.2022.115223>